Precambrian Research, 7 (1978) 349—376

THE LATE PAN-AFRICAN INTRACONTINENTAL LINEAR FOLD BELT OF THE EASTERN HOGGAR (CENTRAL SAHARA, ALGERIA): GEOLOGY, STRUCTURAL DEVELOPMENT, U/Pb GEOCHRONOLOGY, TECTONIC IMPLICATIONS FOR THE HOGGAR SHIELD

J.M.L. BERTRAND[1], R. CABY[1], J. DUCROT[1], J. LANCELOT[1], A. MOUSSINE-POUCHKINE[1] and A. SAADALLAH[2]

[1] *Centre Géologique et Géophysique, Université des Sciences et Techniques du Languedoc, 34060 Montpellier Cedex (France)*
[2] *Département des Sciences de la Terre, Université d'Alger, Alger (Algeria)*

(Received October 11, 1977; revision accepted March 15, 1978)

ABSTRACT

Bertrand, J.M.L., Caby, R., Ducrot, J., Lancelot, J., Moussine-Pouchkine, A. and Saadallah, A., 1978. The Late Pan-African intracontinental fold belt of the Eastern Hoggar (Central Sahara, Algeria): geology, structural development, U/Pb geochronology, tectonic implications for the Hoggar Shield. Precambrian Res., 7: 349—376.

The structural development of the Tiririne Belt, located in the eastern Hoggar, central Sahara, Algeria has been entirely controlled by a high-strain, now vertical, N—S-trending zone, along which metamorphism and deformation gradually appear to the north in the Tiririne Formation, a clastic unit up to 8000 m thick whose sedimentological environment is described. U/Pb geochronology on zircons from a pretectonic sill within the Tiririne Formation indicates a pre-660 Ma depositional age. This intracontinental belt has been formed during the 'late Pan-African', as shown by the 604 and 585 Ma U/Pb zircon ages obtained on syn- to late-kinematic granitic phases from a circular pluton emplaced in the belt (using $\lambda_8 = 0.155125 \cdot 10^{-9}\,y^{-1}$ and $\lambda_5 = 0.98485 \cdot 10^{-9}\,y^{-1}$). The tectonic implications are discussed in the light of the structural and geochronological data. They suggest an eastwards younging of the peak of Pan-African deformation towards the East-Saharan craton, which has been stable for more than 660 Ma.

INTRODUCTION

One of the more conspicuous features of the Hoggar shield is the existence of N—S-trending shear zones interpreted as large-scale transcurrent faults (Caby, 1968).

The shield comprises in its western part a segment of Pan-African age (650—550 Ma), 500 km wide, celled the Pharusian Belt (Caby, 1970) which is mainly composed of Upper Proterozoic calc-alkaline volcanics and plutonics, ultrabasic rocks and volcanic graywackes. Here much evidence points to development in an island-arc type environment (Caby, 1970; Caby et al., 1977) following an oceanic opening between the West African craton and the

Central Hoggar in late Proterozoic times (Caby, 1970; Bertrand and Caby, 1978). In contrast, the Central Hoggar, east of the 4°50′E mega-shear, is mainly composed of older basement rocks, reactivated to varying degrees during the Pan-African orogeny, and narrow schist belts of younger metasediments (Lelubre, 1952; Bertrand, 1974).

This paper, based on recent field work, describes the geological and structural development of an intracontinental linear fold belt controlled by one of the major N–S-trending shear zones of the Eastern Hoggar.

Reconnaissance mapping was carried out in the Eastern Hoggar during the 1960s, after the first synthesis by Lelubre (1952) of the geology of the Hoggar shield, which dealt especially with the Western Hoggar. The most striking feature of the domain, compared with the westernmost part of the shield, is the occurrence of a locally flat-lying and low-grade clastic formation, the Tiririne Formation (Blaise, 1957), extending southwards into Niger, where it was called the Proche Ténéré Formation (Raulais, 1959; Black et al., 1967) and interpreted as the molasse to the Pan-African belt, comparable to the 'Série Pourprée' of the Western Hoggar (Caby and Moussu, 1967). Few detailed studies had previously been carried out and they resulted in two different interpretations: Blaise (1957, 1961) described the Tiririne Formation as a completely independent unit, lying unconformably upon a deeply eroded basement consisting of three distinctive sedimentary and structural environments from the South to the North along the major 8°30′E shear zone. Guérangé and Vialon (1960) on the contrary, because of a misinterpretation of granitic basement (sedimentary cover relationships were interpreted as intrusive contacts), attributed the Tiririne Formation to the 'Pharusian'. They described an eastward prograde tectonic and metamorphic evolution to the eastern Tafassasset and Djanet metasedimentary and metavolcanic formations.

Recent investigations in the Eastern Hoggar have shown that three main longitudinal tectonometamorphic units, separated by rectilinear mylonite zones, can be distinguished (Bertrand and Caby, 1978):

(A) The Temasint-Oumelalen polycyclic domain, including: (i) granulite-facies remnants of Eburnean age (Latouche and Vidal, 1974); (ii) granitic gneisses of older or similar ages, highly reactivated and intruded by Pan-African granites (Picciotto et al., 1965); (iii) metasedimentary gneiss units with Barrovian-type metamorphism, probably equivalent to the Aleksod unit with similar metamorphism, considered as Kibaran by Bertrand (1974) and Bertrand and Lasserre (1976); (iv) monocyclic linear schist belts with greenschist-facies metamorphism of assumed Pan-African age, cut by late to post-kinematic granites.

(B) The Issalane domain comprises a high-grade assemblage consisting of banded and veined granitic to granodioritic gneisses, and a metasedimentary formation characterized by fuschsite-bearing quartzites, calc-silicate gneisses and marbles associated with conformably layered orthogneisses of alkaline affinity. The metamorphism of high-pressure (HP) type is characterized by the presence of rutile in staurolite-kyanite pelitic gneisses and in metabasic rocks. Large-scale migmatisation (associated with low-pressure (LP) high-grade metamorphism?) seems to be superimposed. No age determination is available for the moment, but the rock units are probably pre-Pan-African.

(C) The Tafassasset-Djanet domain or 'East Saharian craton', a pre-Pan-African basement intruded by large batholiths of calc-alkaline granites of unknown age, unconformably overlain by the flat-lying Tiririne formation (Blaise, 1957).

East of Aghergher, this basement comprises low-grade metasediments with chloritoid, and east of Ti-n-Ghoras a marble-calc-silicate sequence, cut by various pretectonic volcanic and plutonic rocks including alkaline gneisses and granites. Semipelitic biotite schists, metaconglomerates and metagraywackes, intruded by sills of metabasalts and metarhyolites, themselves cut by foliated granites, also occur as extremely deformed, vertical N—S-trending shear belts West of Djanet. A main N—S-trending vertical shear zone delimits domains B and C. This major fault of strike-slip type, has controlled the structural evolution of the Tiririne linear fold belt, but we have no proof of its older age and of its direct influence on the depositional conditions of the Tiririne Formation.

LITHOSTRATIGRAPHY AND DEPOSITIONAL ENVIRONMENT OF THE TIRIRINE FORMATION

The Tiririne Formation is separated from its basement by a major unconformity known along the entire Tiririne belt (Fig.1). This unconformity represents the result of sediment deposition upon a palaeo-erosion surface exposing various metamorphic and magmatic rocks of the Djanet-Tafassasset domain. The surface is undulating with locally high-angle slopes and complex relief and is affected by predepositional weathering.

The deposition is probably diachronous and the first sediments are highly variable in composition, depending on the local basement lithology (for example, stromatolite-bearing limestone deposited upon basement marbles southeast of the Kilian erg) and on the local hydrodynamic conditions (high-energy conglomerates, silts and silty limestone in quiet areas, big boulder conglomerates of probable glacial origin).

The Tiririne Formation is exposed to the North within more or less complex synclines in which it reaches a thickness of up to 8000 m. A synthetic log has been defined for each of the synclines (Fig.2). Whilst direct correlations are difficult to establish, sedimentary disconformities allow a subdivision into three units:

Unit I is characterized by clays and carbonates: pelites, silts, silicified dolomites, stromatolite-bearing carbonate lenses, and jaspers.

Unit II sedimentation is almost entirely clastic; the size of clasts is highly variable both laterally and vertically. Polygenic conglomerates of possible glaciogenic origin crop out at the base of this unit (Fig.3 and Plate 1D). One large erratic block about 5 m in length has been observed 10.5 km west-southwest of the SONAREM base, embedded in an arkosic sandstone, ca. 150 m above the basal unconformity. Conglomerates, arkoses, graywackes and silts are arranged in positive sequences (sometimes suggesting Bouma-type sequences) and constitute the main part of the subsident trough of the northern part of the belt. Towards the south limestones with algal laminations and an organic-rich matrix occur at the top of each sequence and are associated with clastic sediments (Plate 1, A and B). These features indicate a tectonically active area of sedimentation (rapid subsidence, synsedimentary faults) where the rate of sedimentation is very high and the material comes from localized source areas.

Unit III, on the contrary, has a more homogeneous lateral development of clastic sediments. The rock types are more mature and red beds appear on top. Sedimentation is not rhythmic and sedimentary structures, including channels, large-scale cross-bedding and ripple marks, are more in agreement with a fluviatile environment, or rather a flood-type deposition upon an area where there exists no differentiation in the deposition processes and their areal distribution.

Palaeogeographic and palaeoclimatological conditions are not clearly understood, although some criteria indicate glacial influence. For Unit II the source seems to be exclusively located to the east, there is no evidence for rock fragments or pebbles from the Western Issalane block. The widely distributed epimetamorphism and cleavage implies deep burial conditions either of sedimentary or tectonic origin.

NATURE AND AGE OF THE PRETECTONIC UPPER PROTEROZOIC IGNEOUS ACTIVITY

Various igneous rocks have intruded the Tiririne Formation. These intrusions are concentrated in the unfolded area south of 22°30′ within the lowermost 1000 m of the sequence.

Fig. 1. Simplified geological map of the Tiririne linear fold belt and adjacent areas.
1. Syn- to post-kinematic granites.
2. Tiririne metasediments of amphibolite-facies grade (a) and anatectic (b).
3. Tiririne Formation: Unit I (a); basal unconformity of Unit II (b); Unit II and III (c); Unit II and III strongly deformed in green-schist facies conditions; (d); pretectonic mainly acidic sills (e).
4. Gneisses and metasediments (a) and late- to post-kinematic intrusions (b) of the Djanet-Tafassasset zone.
5. Issalane block: undifferentiated metasediments and gneisses (and their trend) (a) and idem affected by late Pan-African deformation and retrogressive metamorphism under greenschist-facies grade (b) of the Issalane block.
6. Main shear zones and thrusts.
7. Stretching lineations adjacent to the 8°30′E shear zone in the Issalane block.

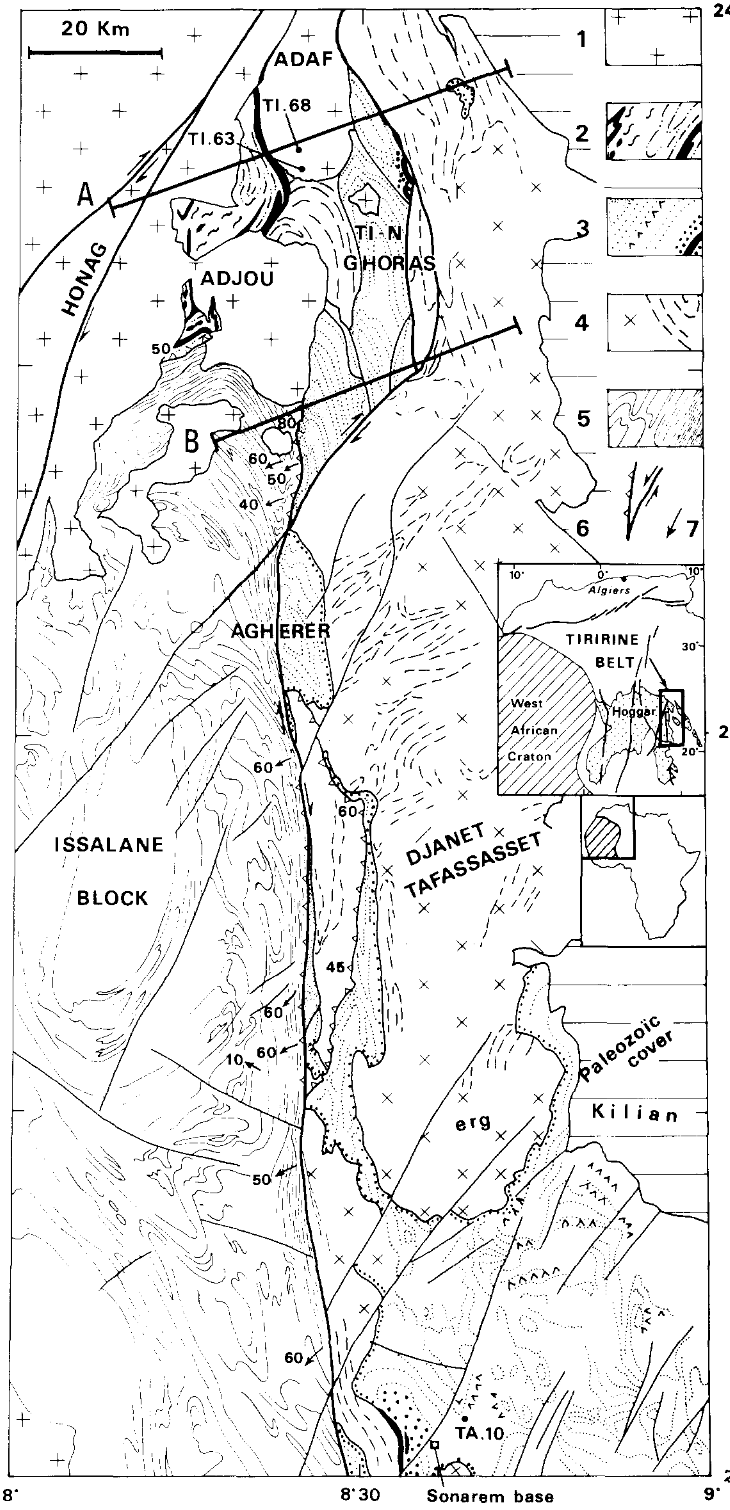

20 Km
ADAF
TI.68
TI.63
A
B
HONAG
ADJOU
TI-N GHORAS
AGHERER
ISSALANE BLOCK
DJANET TAFASSASSET
Paleozoic cover
Kilian
erg
TA.10
Sonarem base
1
2
3
4
5
6
7
Algiers
TIRIRINE BELT
West African Craton
Hoggar
24°
23°
22°
8°
8°30
9°

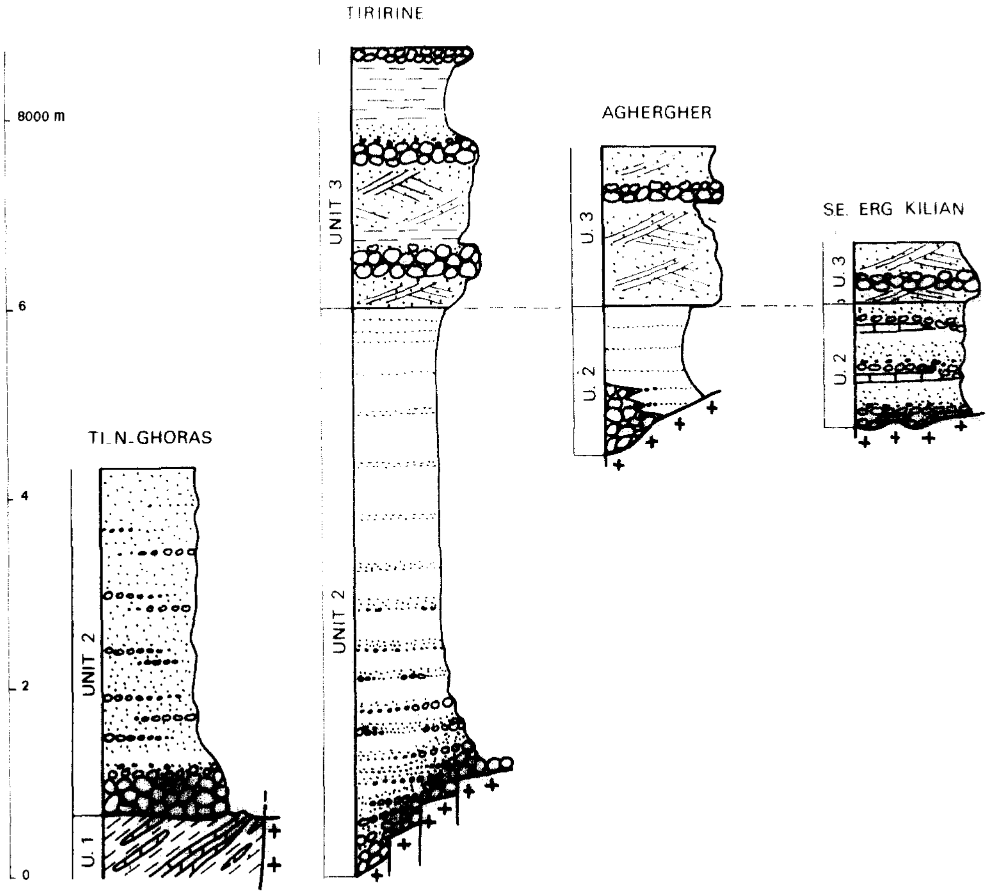

Fig. 2. Schematic logs of the Tiririne Formation.

PLATE 1

A. Flat-lying coarse-grained arkosic sandstone and polygenic conglomerate with carbonate cement, containing some pebbles of limestone from the series itself. Basal part of Unit II, south-east of Erg Kilian.
B. Stromatolite from the lowermost limestone beds resting upon marbles of the Tafassasset-Djanet domain, 50 km south-east of Erg Kilian.
C. Deformation of pebbles disseminated in an abundant green silty matrix under greenschist-facies conditions. Inverted limb of the Tiririne syncline, 500 m from the major thrust. The pebbles are stretched in an E—W direction and are affected by an internal brittle deformation.
D. Conglomerate of possible glacial origin, 1 km west from the SONAREM base. Note the tension veinlets and the interpenetration figures due to pressure solution.
E. Large boulder of granite still preserved in coarse-grained veined gneiss of arkosic origin, southern pendant of the Adjou pluton.
F. Flow folding in a strongly mobilised metatectic gneiss of arkosic origin, northwest of Adjou pluton.

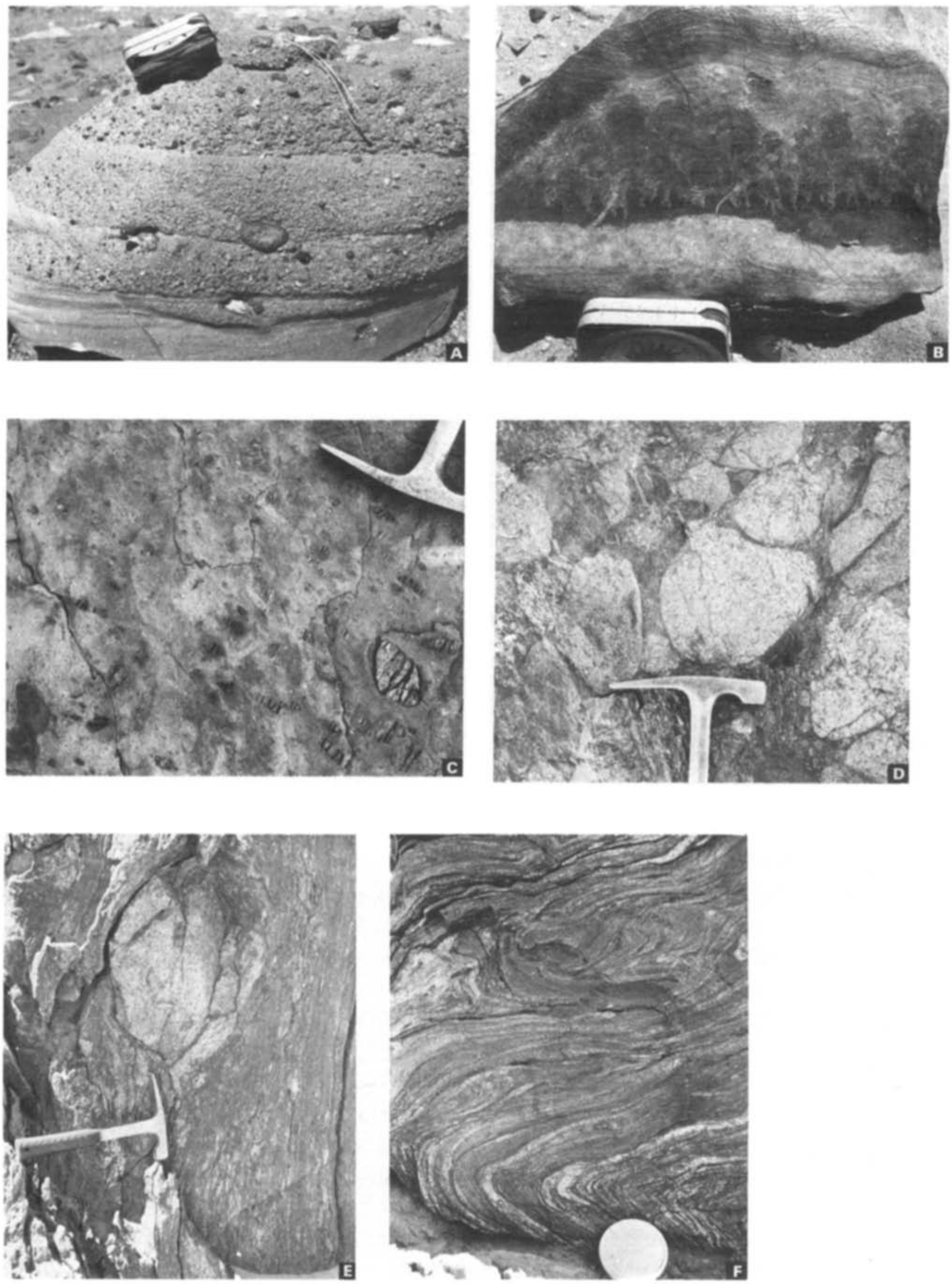
A
B
C
D
E
F

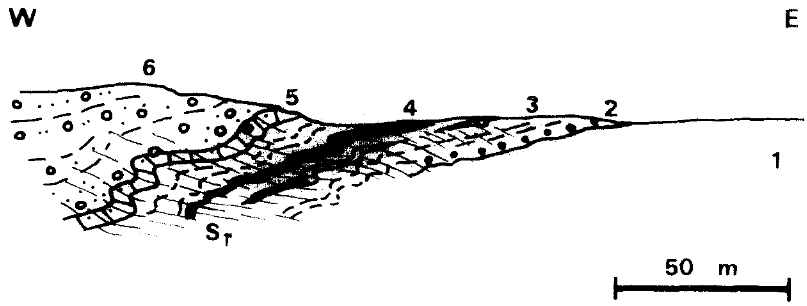

Fig.3. Profile of the basal unconformity 9.5 km south of the SONAREM base.
1. Granodiorite with epidote veinlets, weathered on top.
2. Pebbly arkosic sandstone.
3. Green siltstones and sandstones with some carbonate layers.
4. Microdiorite sill.
5. Limestone and purple siltstones with disseminated boulder on top.
6. Polygenic conglomerate of probable glaciogenic origin with blocks up to 1 m^3. Note the asymetric recumbent folds facing west with associated slaty cleavage.

Different rock types can be distinguished, but their relative chronology is unknown:

(1) Altered olivine gabbros, and layered mafic biotite-diorites forming sills, up to 100 m thick. A few vertical dykes of dark diabases have also been encountered, cutting conglomerates of Unit II.

(2) Often porphyritic acidic lavas, of rhyolitic to rhyodacitic composition, form rare dykes and numerous sills of great extent ($\simeq$ up to 100 km^2) a few metres up to 50 m thick, emplaced in the silty layers of Unit II. No related effusives have been encountered in the investigated area; if present, they must have been emitted much higher in the succession. On the other hand, the red rhyolitic, arkosic sandstones which form Unit III may partly derive from such a volcanic edifice, as is suggested by the occurrence of a rhyolite tuff collected at the bottom of Unit III.

(3) Medium-grained, often leucocratic granodiorites form slightly differentiated sills and oblique dykes. These rocks have suffered an important static recrystallization under greenschist-facies conditions, with development of pistacite, leucoxene, calcite and chlorite. Euhedral zircons have been separated for U/Pb geochronology from an amphibole granodiorite dyke (TA10), 10 m thick, collected from a 35-m-deep borehole in the northern prospect of the Tiririne base (Fig.4).

Three zircon-size fractions have been separated from the TA10 sample. These non-magnetic, euhedral, clear crystals are pink to pale yellow in colour; they generally belong to the S24 type of Pupin and Turco's table (1972, 1975) but P_4 and P_5 types are also present. The three types define the high-temperature field, corresponding to zircons of effusive and monzonitic composition rocks, described by Pupin (1976). Zoning, inherited core, and twinning have not been observed during scanning microscopy and microprobe

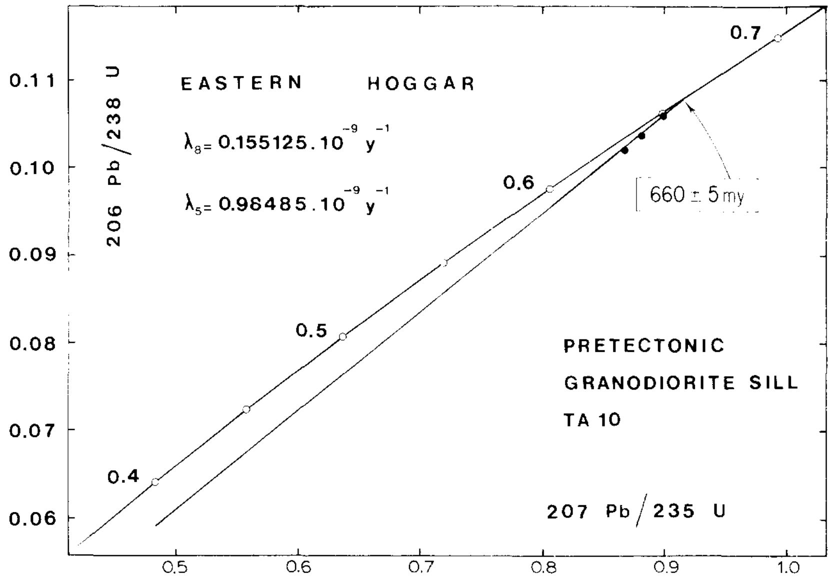

Fig.4. U/Pb Concordia plot of zircon-size fractions data of TA.10 monzonite dyke (Tiririne Formation). Concordia curve is represented and also the upper linear part of a diffusion curve (Tilton, 1960) obtained for a continuous lead loss from 660 Ma to 0.0 Ma. Black spots correspond to measurements.

observations, but some crystals appear fractured and contain some dark silicate inclusions.

The analytical technique has been described (Lancelot et al., 1973, 1976; Lancelot, 1975; Dalmayrac et al., 1977; Ducrot and Lancelot, 1977). The new decay constants, $\lambda_8 = 0.155125 \cdot 10^{-9}$ y^{-1} and $\lambda_5 = 0.98485 \cdot 10^{-9}\, y^{-1}$ (Jaffey et al., 1971) have been used for age determinations. Experimental data are reported in Table I and plotted in the Concordia diagram ($^{206}Pb/^{238}U$–$^{207}Pb/^{235}U$); in this diagram (Fig.4), the experimental points are slightly discordant and define a linear array, the upper intercept with the Concordia curve corresponding to a 660± 5 Ma age. This zircon crystallization age gives an upper limit to the depositional age of the entire Tiririne Formation because some sills also intrude Unit III to the South. One notes that the partial recrystallization of TA10 granodiorite in the greenschist facies has not affected the U/Pb system of zircons (no inherited core, primary crystal typology typical of monzonitic composition, experimental points quite concordant).

STRUCTURE OF THE LINEAR FOLD BELT

The Tiririne linear fold belt is entirely controlled by the 8°30′E shear zone, along which a dynamic-metamorphic gradient affects both basement rocks and the Tiririne Formation. Rectilinear over more than 150 km from the border with Niger, this fault appears to be a major dextral strike-slip fault

TABLE I
Analytical data, granodiorite sill (Tiririne Formation)

Sample	Sample weight (mg)	Size δ (μm)	U (ppm)	Pb (ppm)	($^{206}Pb/^{204}Pb$) meas.*[1]	($^{206}Pb/^{238}U$) corr. *[2]	($^{207}Pb/^{235}U$) corr. *[2]	($^{207}Pb/^{206}Pb$) corr. *[2]
TA10.19	1.28	$80 > \delta > 63$	352	38.6	926	0.10296	0.86687	0.06163
TA10.21	2.35	$125 > \delta > 100$	340	38.6	963	0.10589	0.89841	0.06157
TA10.22	1.33	$160 > \delta > 125$	342	38.5	1222	0.10364	0.88051	0.06165

*[1] meas. = measured.
*[2] corr. = corrected to common lead pollution, with the following measured isotopic composition: $^{206}Pb/^{204}Pb = 17.78$, $^{207}Pb/^{204}Pb = 15.47$, $^{208}Pb/^{204}Pb = 37.49$.

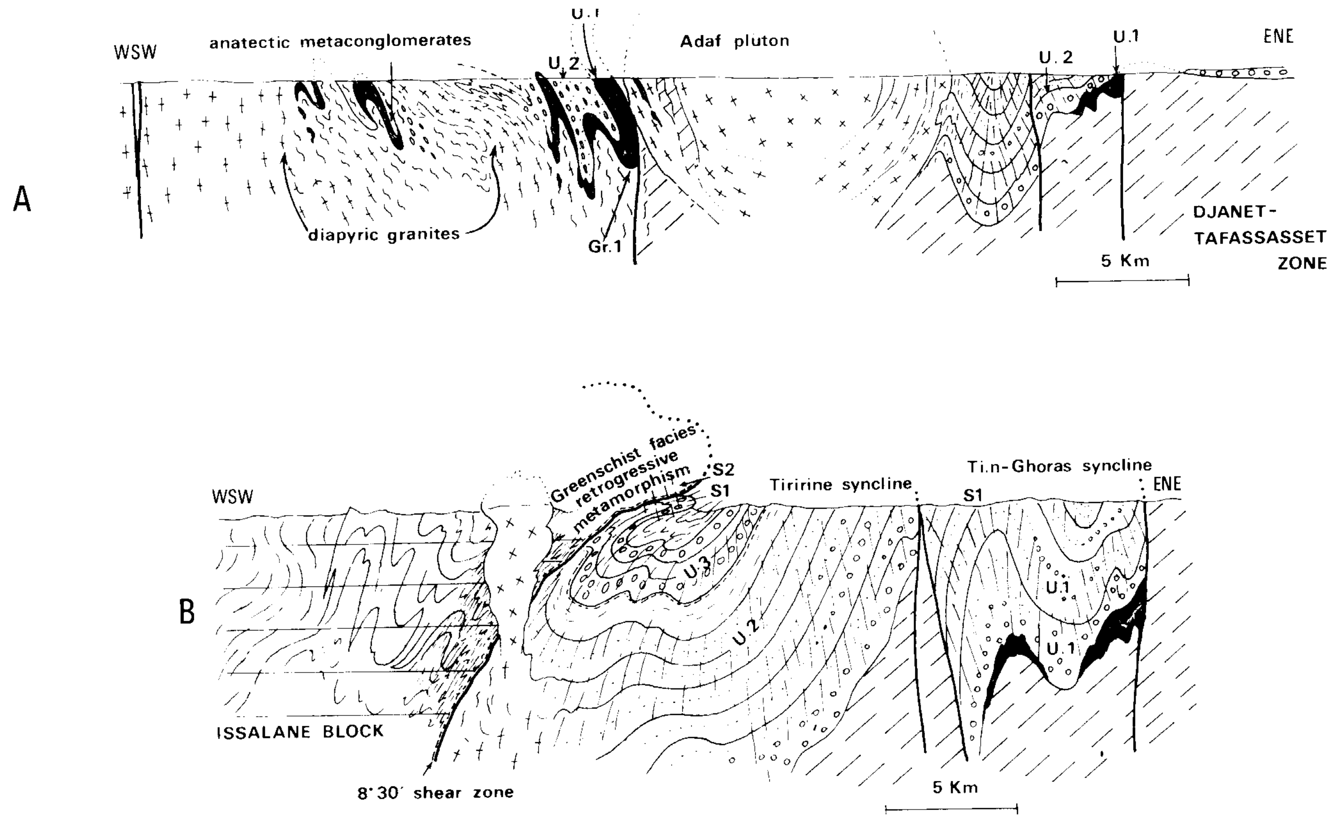

Fig. 5. Two sections across the Tiririne linear fold belt. For location, see Fig. 1. Note the superimposition of S_1 cleavage in the section B along the thrust.

which progressively passes to the North into a thrust (Fig.5). Mylonites and ultramylonites, 20—500 m wide, outline the shear zone. They always exhibit an intense horizontal-stretching lineation (shape of clasts, boudins etc.). Within the Issalane basement a progressive deformation towards the fault can be observed, whereas a post-metamorphic offset of the fault is evidenced South of Aghergher by the low degree of deformation of the Tiririne sediments adjacent to the fault. Further north, one observes the same intensity of deformation and metamorphism in basement rocks and in the sedimentary sequence which is squeezed in narrow belts and synclines. The tectonized zone gradually widens north of 23°15′. Further north, the belt comprises high-grade paragneisses believed to be the metamorphic equivalent of the Tiririne Formation and reactivated basement rocks of B—C zones (see below) cut by large syn-kinematic to post-kinematic granites like the Adaf pluton (see section on radiochronology, p.364).

From south to north, three zones of progressive deformation and metamorphism can be defined in this belt:

Zone A

Zone of flat-lying to slightly folded Tiririne Formation (illite-chlorite zone). South of 22°30′, the Units II and III rest sub-horizontally or are slightly deformed by large dome and basin structures with an amplitude of several kilometres with bedding dips < 10°. A north—south conspicuous subvertical cleavage cuts the strata. Slaty cleavage is developed in the more shaly beds and is outlined by crystallization of illite and chlorite, calcite and iron oxides, whereas the detrital micas are reoriented in the cleavage. The upper greenschist-facies conditions were, however, reached as is evidenced by the blastesis of clinozoisite, pistacite, chlorite, albite, particularly in the green arkosic sandstones and in many of the intrusive rocks. The compact arkosic sandstones show no evidence of deformation, but pressure-solution processes were particularly active, as shown by the very frequent pitted pebbles from the cemented boulder beds and the quartz-epidote tension veinlets in the pebbles. Close to the 8°30′E shear zone, small-size west-facing recumbent folds appear locally (Fig.3). To the North, the Aghergher syncline also belongs to a very hig structural level and shows only a fan-fracture cleavage (Fig.5). NNE-trending normal faults filled by quartz also characterize this zone. Related WNW-trending quartz veins are locally enriched in sulphides and gold. The parental source of these minerals may be represented by pyrite-bearing country rocks (conglomerates and graywackes) or by the basic rocks, which form nearly 50% of intrusive sills in the mineralized district. The global shortening of this zone is negligible.

Zone B

This is a zone with strong deformation under greenschist-facies conditions along the 8°30′ shear zone north of 22°30′. Both the basement rocks of the Issalane and Tafassasset-Djanet domains and synclines of the Tiririne Formation belong to this domain.

New structures and related retrogressive metamorphism in the Issalane basement rocks

Tight folds with N—S axial planes characterize a longitudinal band along the shear zone. These new structures gradually die out to the west, over 10—15 km, but later contact metamorphism, related to numerous post-thrust granite intrusions, obscures these relationships in the northern part, where undeformed andalusite and cordierite occur in pelitic gneisses. The N—S-trending folds of this zone have axial planes dipping west and very variable axes. They may represent both retightened older folds or superimposed folds. The whole of this zone is affected by retrogressive metamorphism that is especially noticeable in altered Al silicates and which increases in intensity but not in grade towards the shear zone. On a smaller scale, porphyroclastic textures are exhibited by all rock types, mostly by reactivation of the well-developed old foliation. The foliation dips to the west and the rocks display a strong stretching lineation parallel to the shearzone plane but with different plunges. From a sub-horizontal trend close to the fault, the lineation progressively turns to a southwest direction as one goes westwards, and is mostly weakly oblique to the mesoscopic fold axes. A peculiar feature is the localisation of a marble and pelitic rock sequence all along the shear zone over more than 60 km. Isoclinally refolded and strongly boudinaged, the marbles exhibit only a newly formed, greenschist-facies assemblage (chlorite, talc, epidote, Fe carbonates, tremolite). The associated chlorite-schists, however, contain augen-shaped clasts of muscovite, kyanite and garnet with rutile inclusions. Some subspherical boudins of metabasic rocks, 10 cm to 1 m in diameter, also contain high-grade mineral relicts such as brown amphiboles, clinopyroxene, garnet and rutile. Within the shear zone itself, the mylonites are often formed at the expense of pelitic gneisses. They still contain augen-shaped or spherical porphyroclasts of various minerals (microcline, kyanite, staurolite, garnet, etc.) embedded in a recrystallized matrix containing newly formed tiny flakes of white mica and brown biotite (Figs.6 and 7). The core of the porphyroclasts contain mineral relicts such as sillimanite needles in K-feldspar and unstrained quartz, and rutile in the garnet. However, the outer rims of the porphyroclasts (garnet with a recrystallized,rim and staurolite) are in equilibrium with the syn-kinematic brown biotite. The occurrence of brown biotite within the shear zone itself contrasting with the chlorite assemblage in the margins, implies a local increase in temperature related to shear-heating.

Structures in the Tiririne Formation

The squeezed syncline along the shear zone. A very narrow synform, a few

Fig.6. Composite mylonite of Issalane rocks within the 8°30'E shear zone at ca. 22°30'N. In the upper part, the clasts are K feldspars and quartz. In the lower part, the clasts of fresh garnet still contain unstrained quartz, brown biotite and rutile inclusions. The matrix is made of quartz, two feldspars and abundant tiny flakes of newly formed brown biotite (× 10).

Fig.7. Mylonitic schist from the same locality. Note here the numerous small clasts of muscovite with oblique cleavage, and the fresh rim of garnet around the garnet clasts. The matrix also contains abundant fresh, minute brown biotite and rare recrystallized fresh staurolite, together with quartz and feldspars (× 10).

hundred metres thick may be followed along the shear zone south of Aghergher over 30 km (Fig.1). The folds are tight to isoclinal, with steep fold axes and vertical axial-plane cleavage. Pebbles of the conglomerates are moderately stretched in a sub-vertical direction parallel to fold axes. The sedimentary features have been obliterated and greenschist-facies syn-kinematic minerals were formed: porphyroblasts of clinozoisite (with a zoisite core), chlorite, albite, minute green biotite and actinolite.

Structure of the Tiririne synclinorium. A rather simple style characterizes this zone, which comprises two simple synclines formed by the > 8000 m thick clastic sediments of Units II and III (Fig.5B). The fan axial-plane cleavage is of fracture type in the compact green arkosic, graywacke and boulder beds of Unit II. A westward increase in deformation is noteworthy, and a slaty cleavage outlined by chlorite and white mica affects the blue-green silt-shales of Unit II. In the overturned western limb of the Tiririne syncline, which dips to the West below the thrusted Issalane unit, the deformation reaches a higher value, as shown by the deformation of the pebbles.

Close to the thrust, the quartz pebbles from a pebbly meta-arkosic sandstone have suffered a N—S elongation parallel to the axis of recumbent folds which face east. The mean ratios of 50 measured pebbles are: 1:2:5. On the other hand, pebbles from a pebbly silty layer affected by intense slaty cleavage 500 m to the East show a predominant flattening related to the sub-horizontal cleavage and have suffered an internal brittle deformation (Plate 1C). A superimposed S_2 fracture cleavage dipping east was subsequently formed close to the thrust.

Zone C

This is a zone with extreme deformation under middle to lower amphibolite-facies conditions. This deeper zone outcrops to the North between large late to post-kinematic Adaf and Adjou granite plutone and a raft within the granites. The gradual passage from meta-arkoses with minute biotite to feldspathic gneisses is only exposed on the northeastern side of the Adaf pluton. The higher-grade metasediments of units I and II only outcrop southwest and northwest of the large Adjou granitic pluton (Figs. 1 and 5A). Unit I is extremely boudinaged on a kilometre scale. The marbles and partly dedolomitized dolomites of the basal sequence of Unit I contain diopside, forsterite, phlogopite, green spinel, talc, ouwarovite, sphene, scapolite . . . and the overlying Mg-Ca-rich sediments have been converted into foliated amphibole-rich rocks containing green hornblende, clinopyroxene, quartz, carbonate, rare Ca plagioclase and sphene. This unit is isoclinally folded. The banded gneisses of arkosic origin (Units I and II?) still contain a few pebbles preserved in a medium-grained porphyroblastic matrix composed of quartz, two feldspars, green biotite ± epidote ± white mica. Going west, remnants of Unit I have been recognized within higher-grade feldspathic gneisses. Extremely tight folds characterize the jaspers associated with the marbles of Unit I, and the quartz-bearing amphibolites contain brown hornblende, greenish clinopyroxene, garnet, ilmenite and rare basic plagioclase. Of special interest is the persistence of large flattened boulders in the partly mobilized feldspathic gneisses of arkosic origin (Plate 1E). Up to 1 m length, their shape mainly depends on the original nature of the rock: pebbles of pegmatite, granite, quartz-diorite, and melanocratic basic rocks with sharp boundaries exhibit a subspherical shape, whereas the other rocks (semibasic rocks, gneisses etc.) are extremely flattened and/or boudinaged into subspherical boudins. The metamorphic differentiation and mobilisation processes responsible for leucocratic mobilisates (and later pegmatites with pink crystals of andalusite) in the more pelitic, non-conglomeratic arkosic gneisses, seem not to have affected the larger pebbles which are preserved, but the smaller ones were probably entirely incorporated into the homogeneous coarse-grained two-mica—two-feldspar ± garnet ± cordierite ± zoisite gneisses by complete pressure and chemical solution.

These rocks show the evidence of polyphase deformation. As they occur only in the western part, close to foliated migmatitic granites emplaced during these high-grade conditions, it is probable that we are dealing with structures without preferred geometry formed during synchronous refolding (Plate 1F). The late folds with NNE trend were formed, however, under lower amphibolite-facies conditions, as indicated by the orientation of most of the minerals and the presence of polygonal arcs of biotite or amphibole in the folds. Southwest of the Adjou pluton, retrogressive conditions are superimposed upon these high-grade conditions and imply a late underthrusting of the Issalane gneisses. Close to this thrust, both units are affected by open to chevron folds with horizontal axial planes, and the rocks of both units exhibit porphyroclastic textures and newly formed minute green biotite.

U/Pb RADIOCHRONOLOGY OF SYN- TO POST-KINEMATIC GRANITE PLUTONS

Numerous granite plutons have been intruded in zone C of the Tiririne fold belt. To the west, the Honag granitic zone, which is cut by a late mylonite zone with a dextral-lateral movement, is clearly post-kinematic with respect to all structures recorded within the Tiririnian fold belt. Even the late underthrusting of the Issalane gneisses below the high-grade metasedimentary gneisses of the Tiririne Formation is affected by retrogressive metamorphism. It is this granite which has yielded a Rb/Sr age of 553 ± 15 Ma (Guérangé and Lasserre, 1971).

Earlier syn-kinematic foliated sheets of porphyritic migmatitic granite with internal flow structures have been emplaced within anatectic gneisses formed at the expense of Tiririne sediments (Fig.8). The Adaf pluton has been selected for radiochronology (Fig.1). It displays both concordant contacts with various gneisses of zone C (Tiririne Formation, Units I and II and

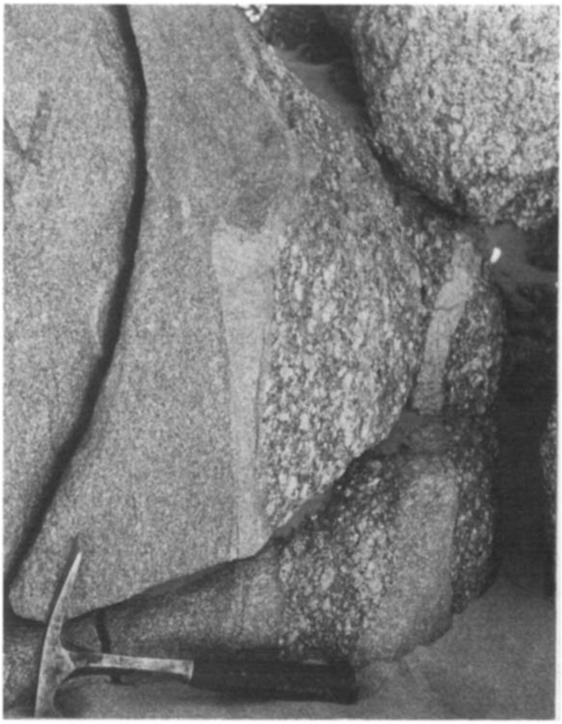

Fig.8. Early syn-kinematic granitic phase, consisting of porphyritic adamellite with fluid structure, medium-grained granite with some biotitic xenoliths and schlieren, and more leucocratic aplites. West Adjou pluton.

its basement to the South) and sharp vein-type contacts to the South-East with pelitic hornfelses of the Tiririne Formation (Units II and III). An internal, more or less helical, circular structure is outlined by different foliated or unfoliated rock types ranging from granite to dark adamellite and hornblende granodiorite, and also by sheets of gneisses belonging to the eastern basement. The foliations have an internal dip, suggesting a deeply eroded ball-like structure. Sheets of syn-kinematic foliated porphyritic granite form the core of contorted flow-folds, whereas various varieties of fine-grained to coarse-grained unoriented granite to granodiorite with some biotite schlieren cut the first-foliated granite with sharp contacts. A post-magmatic penetrative deformation probably related to the late stage of emplacement and to the reactivation of the major shear zones is evidenced by the general cataclasis of quartz, the bending of cleavage planes of biotite, etc. which can be correlated to the blastesis of rare pistacite, chlorite and other deuteric minerals in tension veinlets.

Two samples have been selected for radiochronological analysis to determine the timing of granite emplacement and to compare with the radiometric ages previously obtained on other granites from the rest of the Hoggar.

Ti68

This is a medium-grained foliated adamellite lense included in a porphyritic foliated adamellite considered as syn-kinematic. Rich in minute green biotite and green hornblende, it contains plagioclase phenocrysts with a strong rhythmic zoning mantled by microcline with frequent quartz intergrowths. Sphene and allanite are more abundant than strongly zoned zircon, up to 0.5 mm, which is frequently included in plagioclase (Fig.9). Strained or partly recrystallized quartz and fractures in many phenocrysts resulted from a post-magmatic deformation responsible for the gneissose fabric. This rock can be interpreted as an early magmatic phase subsequently incorporated in the Adaf pluton.

Fig.9. Strongly zoned euhedral zircon, 0.5 mm in length, included in plagioclase, from the medium-grained adamellite Ti68. Note the transverse fractures.

Five zircon-size fractions have been separated from this sample. Euhedral or sub-euhedral crystals belong to S_{18} and to P_4 types in Pupin and Turco's table. For these authors, the two types S_{18} and P_4 are typical of quartz diorite and granodiorite zircons formed at a temperature reaching 800°C.

Ti63

This is a typical porphyritic ademellite with pink microcline phenocrysts and euhedral, strongly zoned plagioclase with a more basic cloudy core mantled by microcline, strained xenocrysts of quartz, green biotite and relicts of pale-green amphibole. Accessories are sphene and zircon, frequently included in biotite. This border facies has been emplaced after the main deformation of the biotite hornfelses, which are cut by veins of the same adamellite.

The euhedral or subeuhedral-zoned zircons belong to S_8, P_2 and G_1 types, typical zircons of anatectic granites emplaced at temperatures of 650—700°C (Pupin and Turco, 1975).

Results of analyses of samples

Scanning microscope and microprobe studies point to the lack of inherited core for the observed zircons of the two samples, but they are commonly fractured and show dark silicate inclusions. Some twinning has also been observed. The analyses have been performed using 1—3 mg weights of zircons.

Experimental data are reported in Table II and plotted in a Concordia diagram ($^{206}Pb/^{238}U$—$^{207}Pb/^{235}U$) (Figs. 10 and 11). For samples Ti68 and Ti63, the zircon-size fractions define a linear array: the upper intercept with the Concordia curve corresponds to a 604±13 Ma age for Ti68 and to a 585±14 m.y. age for Ti63; the lower intercept corresponds to a 76 Ma age for Ti68 and to a 11 Ma age for Ti63. The two latter ages are without geological significance, as no thermal events occurred at these ages, and the episodic lead-loss model of Wetherill (1956) should not be used. The observed linear trends of the experimental points represent the upper linear part of Discordia curves in agreement with continuous lead-loss models (Tilton, 1960; Ulrych, 1963; Wasserburg, 1963).(Figs.10 and 11). It should be noted that the degree of discordancy is clearly correlated with the uranium content, and that this U content itself decreases when the size of zircon fractions increases (Fig.12). These kind of relationships have been described previously by Silver and Deutch (1963) and used by Wasserburg (1963) to define a diffusion lead-loss model with an increasing diffusion coefficient with time (radiation damage in lead-loss model). In comparison with samples Ti63 and Ti68, TA10 zircons present lower U contents (340—350 ppm), corresponding to low degrees of discordancy of the experimental points in the Concordia diagram (Fig.12). Thus, as we consider that the observed linear arrays in the Concordia diagram ($^{206}Pb/^{238}U$—$^{207}Pb/^{235}U$) for samples Ti68 and Ti63 correspond to linear upper parts of Discordia curves, the upper intercepts with the Concordia curve give the zircon crystallization ages, which are 604±13 Ma for the earlier magmatic phase of the Adaf pluton and 585±14 Ma for its post-kinematic part. These ages may be compared to one Rb/Sr isochron age obtained by Guérangé and Lasserre (1971), for the Honag post-kinematic

TABLE II
Analytical data, Adaf pluton

Sample	Sample weight (mg)	Size δ (μm)	U (ppm)	Pb (ppm)	$(^{206}Pb/^{204}Pb)$ meas.*[1]	$(^{206}Pb/^{238}U)$ corr. *[2]	$(^{207}Pb/^{235}U)$ corr. *[2]	$(^{207}Pb/^{206}Pb)$ corr. *[2]
Ti68.19	2.64	$80 > \delta > 63$	1580	127	832	0.06691	0.54515	0.05912
Ti68.20	3.22	$100 > \delta > 80$	1628	137	1178	0.07120	0.58228	0.05934
Ti68.21	2.24	$125 > \delta > 100$	1422	124.5	1261	0.07557	0.61662	0.05921
Ti68.22	3.17	$160 > \delta > 125$	1332	120.6	1183	0.07993	0.65238	0.05923
Ti68.23	3.21	$200 > \delta > 160$	1174	104	3125	0.08333	0.68697	0.05982
Ti63.19	3.10	$63 > \delta > 50$	1749	143	1339	0.07200	0.58874	0.05934
Ti63.19	3.07	$80 > \delta > 63$	1245	106	2241	0.07637	0.62469	0.05935
Ti63.20	3.68	$100 > \delta > 80$	1271	106	2393	0.07630	0.62401	0.05934
Ti63.21	2.17	$125 > \delta > 100$	1118	93	2901	0.08055	0.65898	0.05937

*[1] meas. = measured,
*[2] corr. = corrected to common lead pollution with the following measured isotopic composition:
$^{206}Pb/^{204}Pb = 17.78$, $^{207}Pb/^{204}Pb = 15.47$, $^{208}Pb/^{204}Pb = 37.49$.

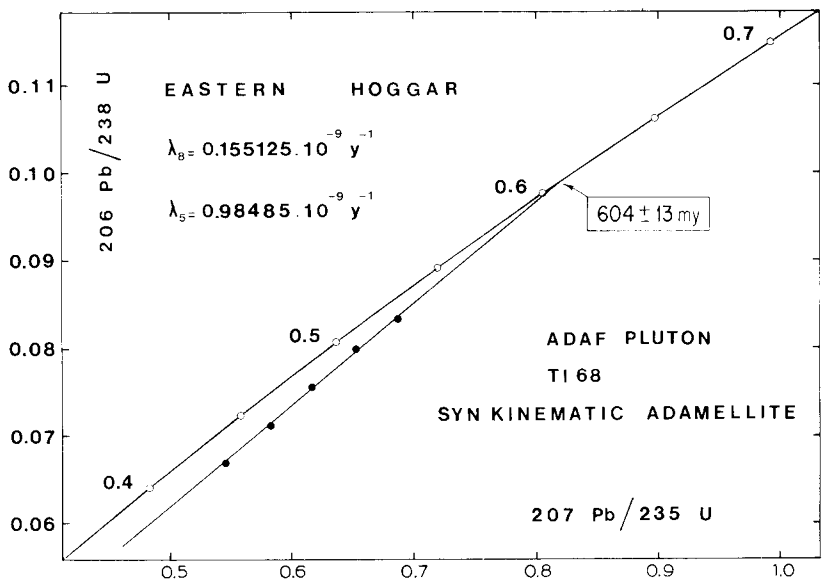

Fig.10. U/Pb Concordia plot of zircon-size fractions data of Ti68 syn-kinematic foliated adamellite (Adaf pluton). Concordia curve is represented, and also the upper linear part of a diffusion curve (Tilton, 1960), obtained for a continuous lead loss from 604 m.y. to 0.0 m.y. Black spots correspond to measurements.

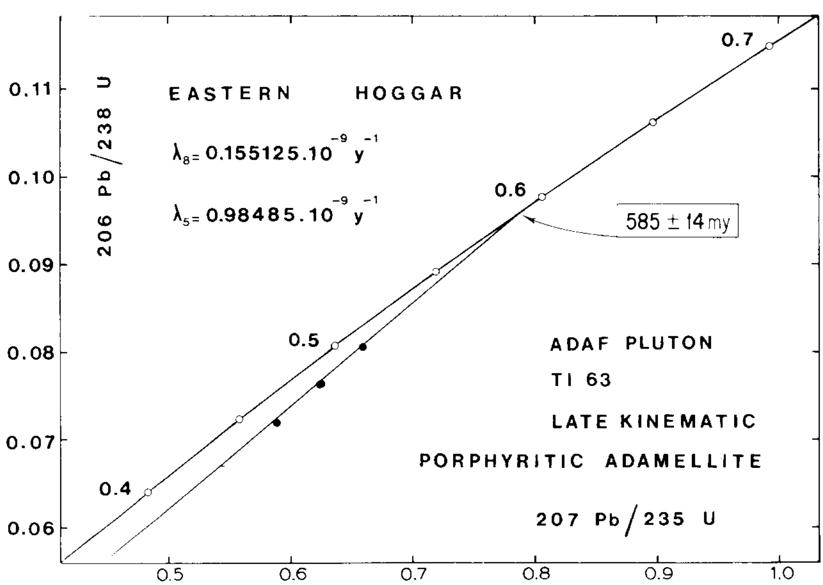

Fig.11. U/Pb Concordia plot of zircon-size fractions data of Ti63 post-kinematic porphyritic adamellite (Adaf pluton). Concordia curve is represented and also the upper linear part of a diffusion curve (Tilton, 1960) obtained for a continuous lead loss from 585 m.y. to 0.0 m.y. Black spots correspond to measurements.

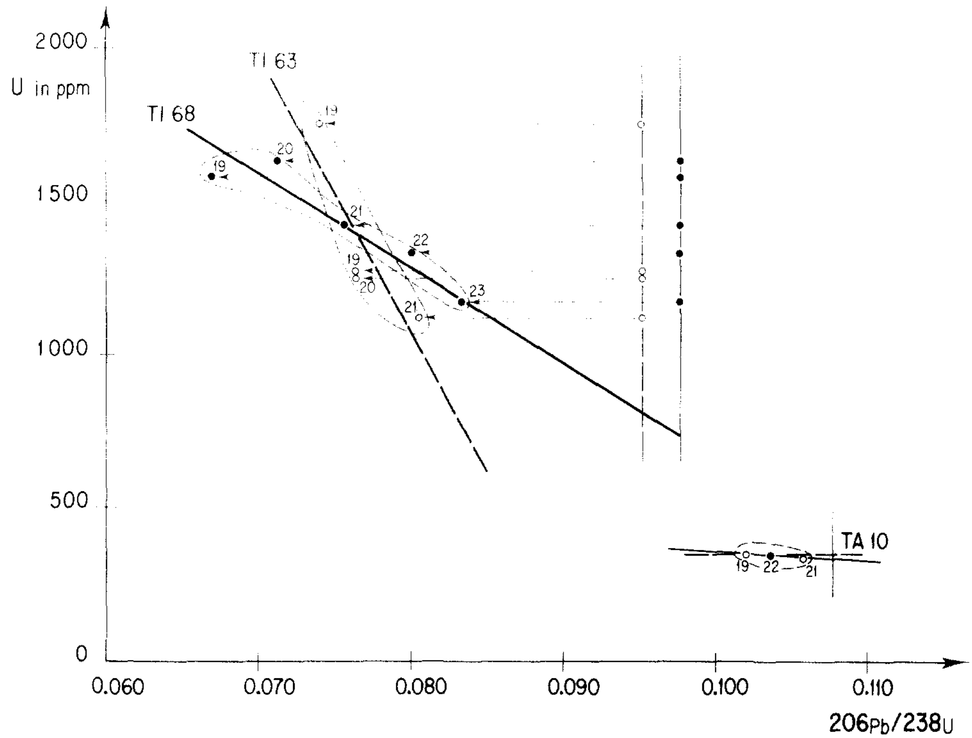

Fig. 12. U content versus $^{206}Pb/^{238}U$ diagram for the three studied samples. Arrows symbolize the degree of discordancy of each size zircon fraction. The starting points correspond to ideal concordant position in a Concordia diagram $^{206}Pb/^{238}U$ — $^{207}Pb/^{235}U$. Note the quite linear correlation between the degree of discordancy and the U content for samples of quite similar ages and also the inverse correlation between the U content and the zircon size.

granite located North of the Issalane domain. Using $\lambda_{87Rb} = 1.42 \cdot 10^{-11}\,y^{-1}$, the recalculated age of this granite is 572±15 Ma.

The U/Pb ages obtained both on pretectonic intrusions and on the Adaf pluton show clearly that both metamorphic and magmatic events which affect the Tiririne belt should be related to the Pan-African orogeny. Late-kinematic diapyric granites of the Taourirt family have also been emplaced in the Pharusian belt of the central Hoggar at ca. 579±40 Ma (Boissonnas et al., 1969) (Age recalculated with $\lambda_{87Rb} = 1.42 \cdot 10^{-11} y^{-1}$). Nevertheless, comparison with previous Rb/Sr and U/Pb ages, obtained on syn-kinematic Pan-African granites from western and central Hoggar with ages in the range of 620—670 Ma (Picciotto et al., 1965; Allègre and Caby, 1972; Bertrand and Lasserre, 1976) seems to indicate a progressive change in time of the main phase of the Pan-African orogeny.

DISCUSSION

The Tiririne Formation is gradually affected, north of 22°15′, by folding and metamorphism. This narrow belt following the 8°30′E shear zone widens northwards and is cut by large plutons of syn- to post-kinematic granites 585—604 Ma old, with some remnants of the same Tiririne Formation preserved inbetween and affected by lower amphibolite-facies conditions and migmatisation. This belt disappears North of the Tafassasset Wadi, sharply cut by two mylonite zones.

The rather simple structure of this belt may have developed as follows (Fig.13):

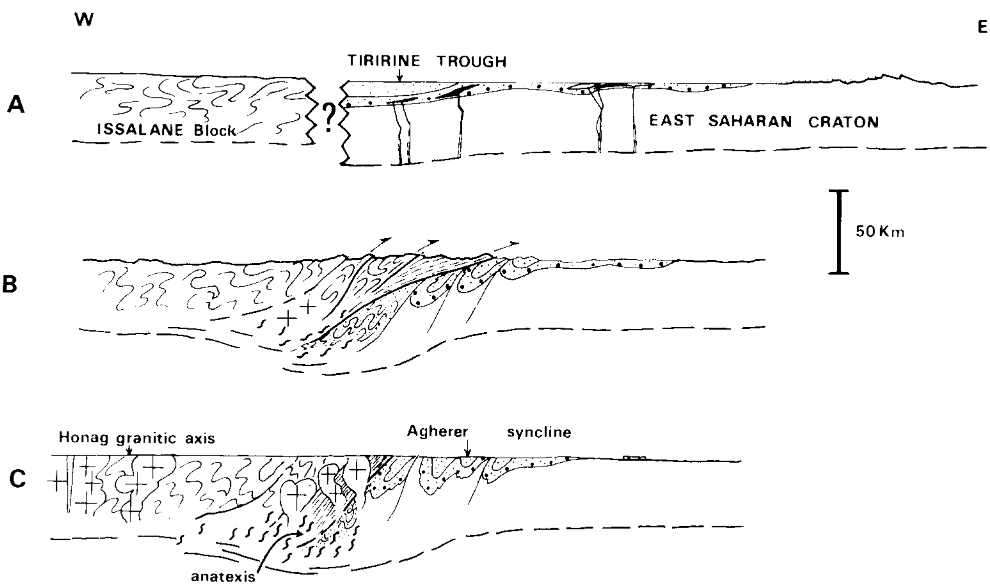

Fig.13. Tectonic evolution of the Tiririne belt, schematized in three stages.

(1) The Tiririne Formation. Both the ensialic sedimentary environment and the molassic affinities of the upper part of the sequence imply the destruction of reliefs located to the east of the subsiding zone. It is important to notice the longitudinal variations along the 8°30′ lineament: the thickness of the sedimentary pile is greater to the North where the subsequent deformation and metamorphism were the more important. The depositional age of the formation is, however, still unknown but predates the 660 Ma old igneous event. There is a striking similarity between the green polygenic conglomerates and the green-banded silts of Unit II and the late Proterozoic 'série verte' of the Western Hoggar (Caby, 1970). On the other hand, the glacial conglomerates and the associated organic-rich limestones of the molassic 'série pourprée' in the same area (Caby and Moussu, 1968) are also

lithologically very comparable to some beds of Unit II, south of 22°30′.

(2) Pretectonic magmatism took place in a continental environment ca. 660 Ma ago in the stable area in the form of acidic and basic sills. Mafic diorite and gabbros may imply a direct contribution from the upper mantle, whereas the acidic rocks (rhyolites), which contain dark basic xenoliths, may have a later deep crustal source.

(3) The presence of a vertical cleavage in the flat-lying Tiririne Formation, less than 1500 m thick in the Tafassasset-Djanet area, implies that at least 5000 m of overlying sediments have also covered the stable eastern domain and that a negligible shortening of this cratonic domain may be correlated with a slight sub-vertical extension of the sedimentary cover.

(4) On a global scale, we suggest that initially an E—W collision occurred between the stable eastern cratonic domain of the Tafassasset-Djanet domain and the rest of the already uplifted eastern Pan-African belt, which is mostly composed of reactivated pre-Pan-African basement rocks (Bertrand and Caby, 1978). The geometry of the rapidly subsiding longitudinal trough filled by sediments of the Tiririne Formation, the sialic basement of which was certainly buried below at least 10 km of overlying sediments, induced the overthrusting of the Issalane pre-Pan-African basement rocks, and synthetic thrusts in the foreland (Fig.13B). This intracontinental megashear, which sharply delimits the Tiririne belt to the West, indicates an extreme deformation related to this E—W collision. The E—W crustal shortening in the frontal part of the Issalane basement unit may have involved a thickening of the crust, subjected at depth to low-pressure melting conditions giving way to the syn-tectonic granitoid magmas. The Honag granitic zone may also be the result of the same melting event occurring along another backward shear zone.

(5) As the collision was going on, the thrust plane progressively straightened and steepened and the thrust movement evolved to a strike-slip movement along the same fault plane (Fig.13C). Such a dextral transcurrent movement may explain the steeply plunging folds in the narrow belt of highly deformed Tiririne sediments, and its close juxtaposition with only slightly deformed beds of the Aghergher syncline.

(6) At a late stage of the same collision, second-order dextral strike-slip faults are superimposed upon the thrust plane, south of the Tiririne syncline. The northern underthrusting of the Issalane basement unit below the retrogressed and mylonitized lower amphibolite-facies rocks of the Tiririne Formation, would also fit with this late stage of collision which was responsible for a dextral confrontation of the two colliding zones.

(7) The 8° 30′E shear which to the West bounds the Tiririne fold belt does not represent the original western margin of the upper Proterozoic basin, but only possesses the characteristics of a syn-tectonic shear zone. Concerning the possible amount of shortening between the Issalane pre-Pan-African basement and the linear Tiririne belt, and the original width of the Tiririne basins, we point out the following evidence:

(a) Taking into account the fold structures and the latest dextral strike-slip faults superimposed on the 8°30′E shear north of the Aghergher syncline, the original width of the Tiririne trough can be estimated to have been at least ca. 50 km. The western part, only exposed to the North, affected by a low-pressure/ high-temperature metamorphism and by extreme deformation, accounts for at least 25—30 km of an initial overthrusting of the Issalane pre-Pan-African basement upon the Tiririne belt at an early stage of the tectonic development (Fig. 13B). During this early stage, deep synthetic thrusting affecting the lower crust would have caused anatexis and granite collection and emplacement within both the basement rocks and within the Tiririne metasediments, consecutively to a global crustal thickening due to the superposition of the Issalane crust upon the East-Saharan crust.

(b) Though no systematic lineation measurements have been made within and along the 8°30′E shear zone, it appears that the horizontal lineation within the shear zone accounts for the extreme horizontal shearing, the dextral sense of which has been proven in the field by small-scale dextral displacements, and by the orientation of the oblicity of the foliation in zones of progressive deformation. The SW—NE steep-stretching lineation represents the direction of tectonic transport at a high angle to the shear-zone itself. The more ductile Tiririne metasediments exhibit alternative zones of vertical or horizontal maximum elongation. These facts suggest that the relative rigidity of the East-Saharan craton has induced a lateral expulsion of the deformed materials of the Tiririne Formation along the shear zone, both vertical and horizontal, according to the areas, even though the maximum compression acting in the Issalane unit was SW—NE with a southwestwards dip.

We also tentatively correlate the late Pan-African granitic plutons emplaced in the Issalane basement unit with the melting processes operative at depth in the inferred thickened crust related to this fold belt. Structurally the Tiririne linear fold belt is characterized over more than 150 km by the overall horizontal stretching and mineral lineations co-axial with fold axes within a narrow belt a few hundred metres wide, where extreme deformation responsible for mylonites took place. Within the shear zone, shear heating locally allowed the blastesis of brown biotite and fresh staurolite. This linear fold belt fits well into the general interpretation of continental shear zones (Nicolas et al., 1977) though upwelling of granitic and anatectic rocks, and later diapirism of granites formed at depth, obscure the general pattern in the northern part of the belt.

Tectonic implications for the Hoggar shield

The maximum width of the East Saharan craton does not exceed 700 km, since recent data indicate that other linear belts with granites of the same age occur in the Tibesti mountains (Pegram et al., 1976). The 8°30′E shear zone may represent its actual highly deformed and down-going western margin, along which the Tiririne belt developed. Compared with the Pharusian belt of central-Western Hoggar, we must emphasize its complete ensialic character and the lack of calc-alkaline volcanics. We have argued that the 8°30′E shear zone has actually the characteristics of a syn- to late-tectonic structure, and we suggest a similar origin for many of the other shear zones and associated shear belts of the Hoggar previously considered as the original pretectonic border zones of upper Proterozoic basins or troughs. Lastly, the N—S shear belts and shear zones which can be pre-Pan-African in the Djanet-Tafassasset domain, are Pan-African *s.s.* (650—580 Ma) in central-western Hoggar, and late Pan-African (ca. 580 Ma and younger) along the Tiririne belt. This diachronism suggests an eastward shift of the main phase of the Pan-African orogeny across the Hoggar.

ACKNOWLEDGEMENTS

We gratefully acknowledge financial support from the Centre National de la Recherche Scientifique and from the Department of Geology of the University of Algiers and SONAREM. Thanks are due to Dr E. Ball, Dr J. Fabre, Dr Y. Mahdjoub, Dr P. Riffault and Dr K. Zellouf for their field contribution in 1975 and to Dr J. Blaise for letting us have access to his unpublished field data. Comments from Dr R. Black improved the presentation and the English text.

REFERENCES

Allègre, C.J. and Caby, R., 1972. Chronologie absolue du Précambrien de l'Ahaggar occidental. CR Acad. Sci. Paris, 275: 2095—2098.

Bertrand, J.M.L., 1974. Evolution Polycyclique des GneissPrecambriens de l'Aleksod (Hoggar Central, Sahara Algérien). Aspects Structuraux, Pétrologiques, Géochimiques et Géochronologiques. Thèse Etat, Univ. Montpellier. CNRS (CRZA), Sér. Géol., 19: 350 pp.

Bertrand, J.M.L. and Caby, R., 1978. Geodynamic evolution of the Pan-African orogenic belt: a new interpretation of the Hoggar shield. Geol. Rundsch., 67(2).

Bertrand, J.M.L. and Lasserre, M., 1976. Pan-African and pre-Pan-African history of the Hoggar (Algerian Sahara) in the light of new geochronological data from the Aleksod area. Precambrian Res., 3: 343—362.

Black, R., Jaujou, M. and Pellaton, C., 1967. Carte Géologique du Massif de l'Air (1/500 000e). Notice Explicative. BRGM, 57 pp.

Blaise, J., 1957. Une 'Série Intermédiaire' au Sahara central: la série de Tiririne (Ahaggar oriental). In: Les Relations entre Précambrien et Cambrien. Coll. Int. CNRS, Paris, pp. 217—222.

Blaise, J., 1961. Sur la stratigraphie des séries anté-cambriennes dans la région du Tafassasset moyen (Ahaggar oriental). Bull. Soc. Geol. Fr., III: 184.

Boissonnas, J., Borsi, S., Ferrara, G., Fabre, J., Fabries, J. and Gravelle, M., 1969. On the early cambrian age of two late orogenic granites from West-central Ahaggar (Algerian Sahara). Can. J. Earth Sci., 6: 25—37.

Caby, R., 1968. Une zone de décrochements à l'échelle de l'Afrique dans le Précambrien de l'Ahaggar occidental. Bull. Soc. Géol. Fr., X: 577—587.

Caby, R., 1970. La Chaine Pharusienne dans le Nord-Ouest de l'Ahaggar (Sahara Central, Algérie); sa Place dans l'Orogenèse du Précambrien Supérieur en Afrique. Thèse Univ. Sci. Montpellier and Serv. Carte Géol. Algérie, in press.

Caby, R. and Moussu, H., 1967. Une grande série détritique du Sahara: stratigraphie, paléogéographie et évolution structurale de la "Série pourprée" dans l'Aseg'rad et le Tanezrouft oriental (Sahara algérien). Bull. Soc. Géol. Fr., IX: 876—882.
Caby, R., Dostal, J. and Dupuy, C., 1977. Upper proterozoic volcanic graywackes from north-western Hoggar (Algeria). — Geology and geochemistry. Precambrian Res., 5: 283–297.
Dalmayrac, B., Lancelot, J. and Leyreloup, A., 1977. 2 b.y. granulites in the Late Precambrian metamorphic basement along the southern Peruvian coast. Science, 198: 49—51.
Ducrot, J. and Lancelot, J., 1977. Problème de la limite Précambrien-Cambrien. Etude radiochronologique par la méthode U/Pb sur zircons du volcan du Jbel Boho (Anti-Atlas marocain). Can. J. Earth Sci., 14(12): 2771—2777.
Guérangé, B. and Vialon, P., 1960. Le Pharusien du bassin de Djanet dans la région du Tafassasset moyen (Ahaggar oriental, Sahara central). CR Somm. Soc. Géol.Fr., 3: 57—59.
Guérangé, B. and Vialon, P., 1962. Le Pharusien du Tafassasset moyen. Ses relations avec le Suggarien de la zone d'Issalane. Trav. Inst. Rech. Sahar. Algér., 21: 7—56.
Guérangé, B. and Lasserre, M., 1971. Etude géochronologique de roches du Hoggar oriental par la méthode au strontium. CR Somm. Soc. Géol. Fr., 4: 213—215.
Jaffey, A.H., Flynn, K.F., Glendenin, L.E., Bentle, E.C. and Essling, A.M., 1971. Précision measurement of half lives and specific activities of ^{235}U and ^{238}U. Phys. Rev., C4 (5): 1889—1906.
Lancelot, J.R., 1975. Les systèmes U/Pb: Chronomètres et Traceurs de l'Évolution des Roches Terrestres. Thèse, Univ. Paris VII.
Lancelot, J.R., Vitrac, A. and Allegre, C.J., 1973. Datation U/Th/Pb des zircons grain par grain, par dilution isotopique. Conséquences géologiques. CR Acad. Sci. Paris, 277(D): 2117—2120.
Lancelot, J.R., Vitrac, A. and Allegre, C.J., 1976. Uranium and lead isotopic dating with grain by grain zircon analysis: a study of complex geological history with a single rock. Earth Planet. Sci. Lett., 29: 357—366.
Latouche, L. and Vidal, Ph., 1974. Géochronologie du Précambrien de la région des Gour Oumelalen (Nord-Est de l'Ahaggar, Algérie). Un exemple de mobilisation du strontium radiogénique. Bull. Soc. Géol. Fr., (7)14: 195—203.
Lelubre, M., 1952. Recherches sur la géologie de l'Ahaggar central et occidental (Sahara central). Bull. Serv. Carte Géol. Algér., 2e série, no.22.
Nicolas, A., Bouchez, J.L., Blaise, J. and Poirier, J.P., 1977. Geological aspects of plasticity in continental shear zones. Tectonophysics, 42: 55—73.
Pegram, W.J., Register, J.L., Fullagar, P.D., Ghuma, M.A. and Rogers, J.J.W., 1976. Pan-African ages from a Tibesti massif batholith, Southern Libya. Earth Planet Sci. Lett., 30: 123—128.
Picciotto, E., Ledent, D. and Lay, C., 1965. Etude géochronologique de quelques roches du socle cristallophyllien du Hoggar. Proc. 151st Coll. Int. CNRS Géochron. Abs. Nancy, pp. 277—289.
Pupin, J.P., 1976. Signification des Caractères Morphologiques du Zircon Commun des Roches en Pètrologie. Bases de la Méthode Typologique. Applications. Thèse, Univ. Nice, 393 pp.
Pupin, J.P. and Turco, G., 1972. Application des données morphologiques du zircon accessoire en pétrologie endogène. CR Acad. Sci. Paris, 275 (D): 799—802.
Pupin, J.P. and Turco, G., 1975. Typologie du zircon accessoire dans les roches plutoniques dioritiques, granitiques et syénitiques. Facteurs essentiels déterminant les variations typologiques. Pétrologie, I(2): 139—156.
Raulais, M., 1959. Esquisse géologique sur le massif cristallin de l'Air (Niger). Bull. Soc. Géol. Fr., (7)I: 207—223.

Silver, L.T. and Deutsch, S., 1963. Uranium lead isotopic variations in zircons: a case study. J. Geol., 71: 721—729.
Tilton, G.R., 1960. Volume diffusion as a mechanism for discordant Pb ages. J. Geoph. Res., 65: 2933—2937.
Ulrych, T.J., 1963. Discordant lead uranium ages due to the continuous loss of lead. Nature, 200: 561—562.
Vitrac, A., Lancelot, J.R., Allegre, C.J. and Moorbath, S.S., 1977. U-Pb ages on single zircons from the Early Precambrian rocks of West Greenland and the Minnesota River Valley. Earth Planet. Sci. Lett., 35: 449—453.
Wasserburg, G.J., 1963. Diffusion processes in Pb-U systems. J. Geophys. Res., 68: 4823—4846.
Wetherill, C.W., 1956. Discordant U Pb ages. Trans. Am. Geophys. Union, 37: 320—326.